Syntheses of Pyrimidine-Based Polymers Containing Electron-Withdrawing Substituent with High Open Circuit Voltage and Applications for Polymer Solar Cells

Juae Kim,[1] Joo Young Shim,[1] Jihoon Lee,[2] Dal Yong Lee,[2] Sangmin Chae,[3] Jinwoo Kim,[1] Il Kim,[4] Hyo Jung Kim,[3] Sung Heum Park,[2] Hongsuk Suh[1]

[1]Department of Chemistry and Chemistry Institute for Functional Materials, Pusan National University, Busan 609-735, Korea
[2]Department of Physics, Pukyong National University, Busan 608-737, Korea
[3]Department of Organic Material Science and Engineering, Pusan National University, Busan 609-735, Korea
[4]Department of Polymer Science and Engineering, Pusan National University, The WCU Center for Synthetic Polymer Bioconjugate Hybrid Materials, Busan 609-735, Korea
Correspondence to: H. Suh (E-mail: hssuh@pusan.ac.kr)

Received 25 June 2015; accepted 28 August 2015; published online 10 October 2015
DOI: 10.1002/pola.27910

ABSTRACT: Polymers using new electron-deficient units, 2-pyriminecarbonitrile and 2-fluoropyrimidine, were synthesized and utilized for the photovoltaics. Donor-acceptor (D-A) types of conjugated polymers (**PBDTCN, PBDTTCN, PBDTF,** and **PBDTTF**) containing 4,8-*bis*(2-octyldodecyloxy)benzo[1,2-*b*;3,4-*b*′]dithiophene (BDT) or 4,8-*bis*(5-(2-octyldodecyloxy)thiophen-2-yl)benzo[1,2-*b*:4,5-*b*′]dithiophene (BDTT) as electron rich unit and 2-pyriminecarbonitrile or 2-fluoropyrimidine as electron deficient unit were synthesized. We designed pyrimidine derivatives in which strong electron-withdrawing group (C≡N or fluorine) was introduced to the C2 position for the generation of strong electron-deficient property. By the combination with the electron-rich unit, the pyrimidines will provide low band gap polymers with low highest occupied molecular orbital (HOMO) energy levels for higher open-circuit voltages (V_{OC}). For the syntheses of the polymers, the electron-rich and the electron-deficient units were combined by Stille coupling reaction with Pd(0)-catalyst. Absorption spectra of the thin films of **PBDTTCN** and **PBDTTF** with BDTT unit show shift to a longer wavelength region than **PBDTCN** and **PBDTF** with BDT unit. Four synthesized polymers provided low electrochemical bandgaps of 1.56 to 1.96 eV and deep HOMO energy levels between −5.67 and −5.14 eV. © 2015 The Authors. Journal of Polymer Science Part A: Polymer Chemistry Published by Wiley Periodicals, Inc. J. Polym. Sci., Part A: Polym. Chem. **2016**, *54*, 771–784

KEYWORDS: conducting polymers; high performance polymers; structure-property relations

INTRODUCTION For the polymer solar cells (PSCs), the bulk heterojunction structure has been examined intensively over the past decades especially caused by their features such as low cost, light weight, flexibility, and the possibility of large area fabrication by loll-to loll process.[1,2]

D-A type of polymers are advantageous for the construction of efficient low band gap polymers with extended long wavelength absorption and reduced HOMO energy level for the enhancement of open-circuit voltage (V_{OC}).[3]

Benzo[1,2-*b*:4,5-*b*′]dithiophene (BDT) is one of the best electron-rich sub-structure, due to the rigid and coplanar fused ring system, for (i) the enhancement of π-stacking, hole mobility and extended π-conjugated system and (ii) the introduction of suitable side chain for better solubility. BDT-based copolymers have been reported to provide PSCs with PCE values up to 9%.[3–6]

Many types of electron-deficient units, including 2,1,3-benzothiadiazole,[7] diketopyrrolo[3,4-*c*]-pyrrole-1,4-dione,[8] and thieno[3,4-*c*]pyrrole-4,6-dione,[9] have been reported for the D-A type of low band-gap polymers.[10] Among them, compounds containing pyrimidine unit have been studied as promising materials to present a compact stacking for high mobility owing to coplanar conformation. However, there have not been many reports on copolymers with pyrimidine for organic solar cells (OSCs).[11–13]

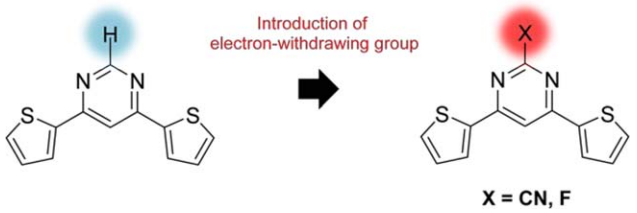

FIGURE 1 Approach towards new electron-deficient moiety. [Color figure can be viewed in the online issue, which is available at wileyonlinelibrary.com.]

To craft efficient electron-deficient moiety, we designed pyrimidines in which strong electron-withdrawing group (C≡N or fluorine) was introduced to its C2 position, which will lead to low band gap polymers for PSCs as shown in Figure 1.[3,11] In case of pyrimidines in which C≡N or fluorine was introduced, the cyano group and fluorine groups are strong acceptor units to provide properties of higher conjugation, coplanarity, and rigidity.[6,11]

In this article, we report D-A types of conjugated polymers, **PBDTCN, PBDTTCN, PBDTF,** and **PBDTTF**, containing BDT or BDTT as donor (D) unit and 2-pyriminecarbonitrile or 2-fluoropyrimidine as acceptor (A) unit (Schemes 1 and 2).[14,15]

By using the Stille coupling condition, BDT/BDTT and 2-pyriminecarbonitrile/2-fluoropyrimidine fragments were incorporated to synthesize poly(4,6-*bis*(4-hexyl-2-thienyl)-2-pyrimidinecarbonitrile-*alt*-4,8-di(2-octyldodecyloxy)benzo[1,2-*b*;3,4-*b*′]dithiophene) (**PBDTCN**), poly(4,6-*bis*(4-hexyl-2-thienyl)-2-pyrimidinecarbonitrile-*alt*-4,8-*bis*(5-(2-octyldodecyloxy)thiophen-2-yl)benzo[1,2-*b*:4,5-*b*′]dithiophene) (**PBDTTCN**), poly(4,6-*bis*(4-hexyl-2-thienyl)-2-fluoropyrimidine-*alt*-4,8-di(2-octyldodecyloxy)benzo [1,2-*b*;3,4-*b*′]dithiophene) (**PBDTF**), and poly(4,6-*bis* (4-hexyl-2-thienyl)-2-fluoropyrimidine-*alt*-4,8-*bis*(5-(2-octyldodecyloxy)thiophen-2-yl)benzo[1,2-*b*:4,5-*b*′]dithiophene) (**PBDTTF**). Novel conjugated polymers showed good solubility at room temperature in various organic solvents. The photovoltaic properties of the polymers were investigated by

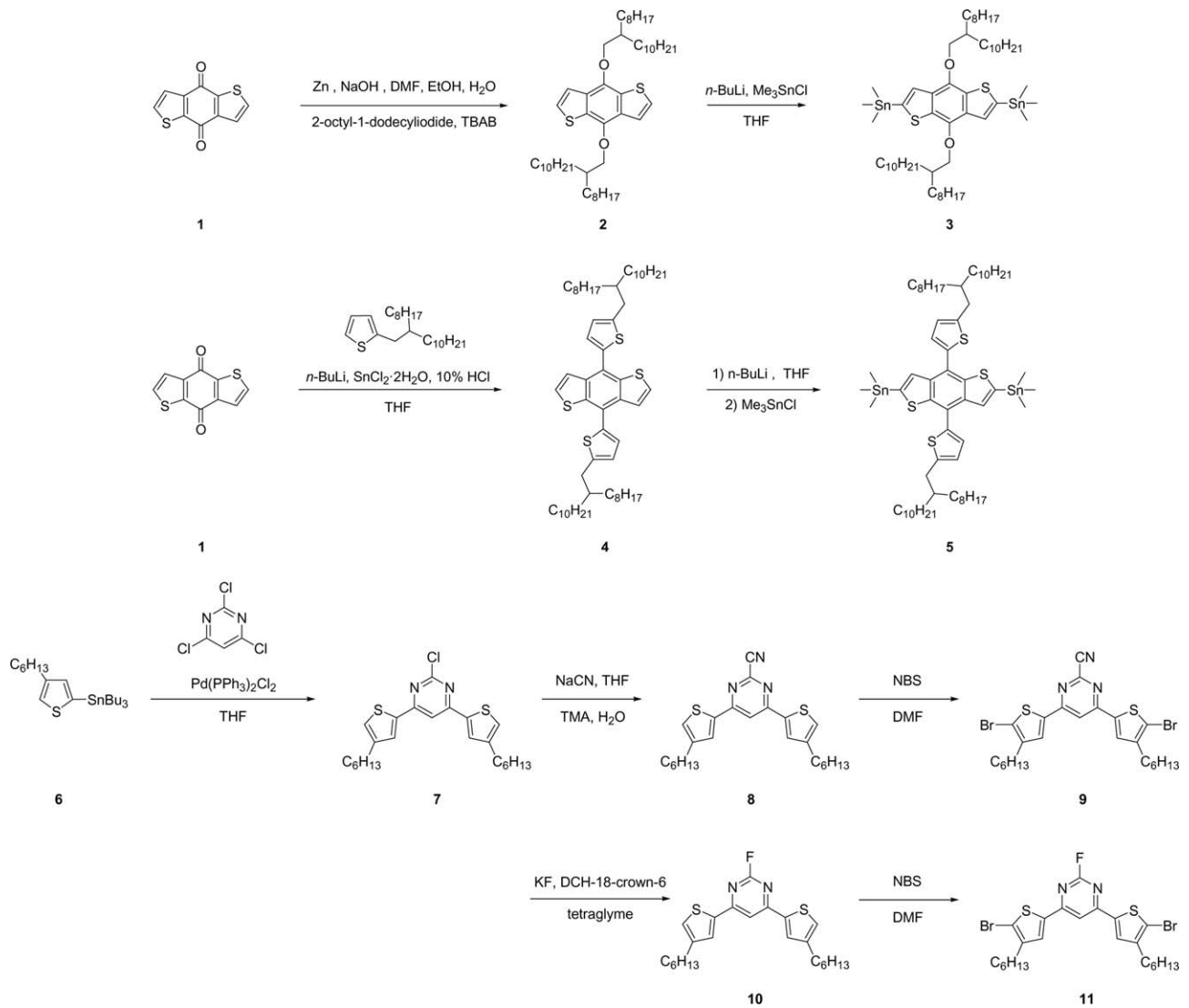

SCHEME 1 Synthetic route for the syntheses of the monomers.

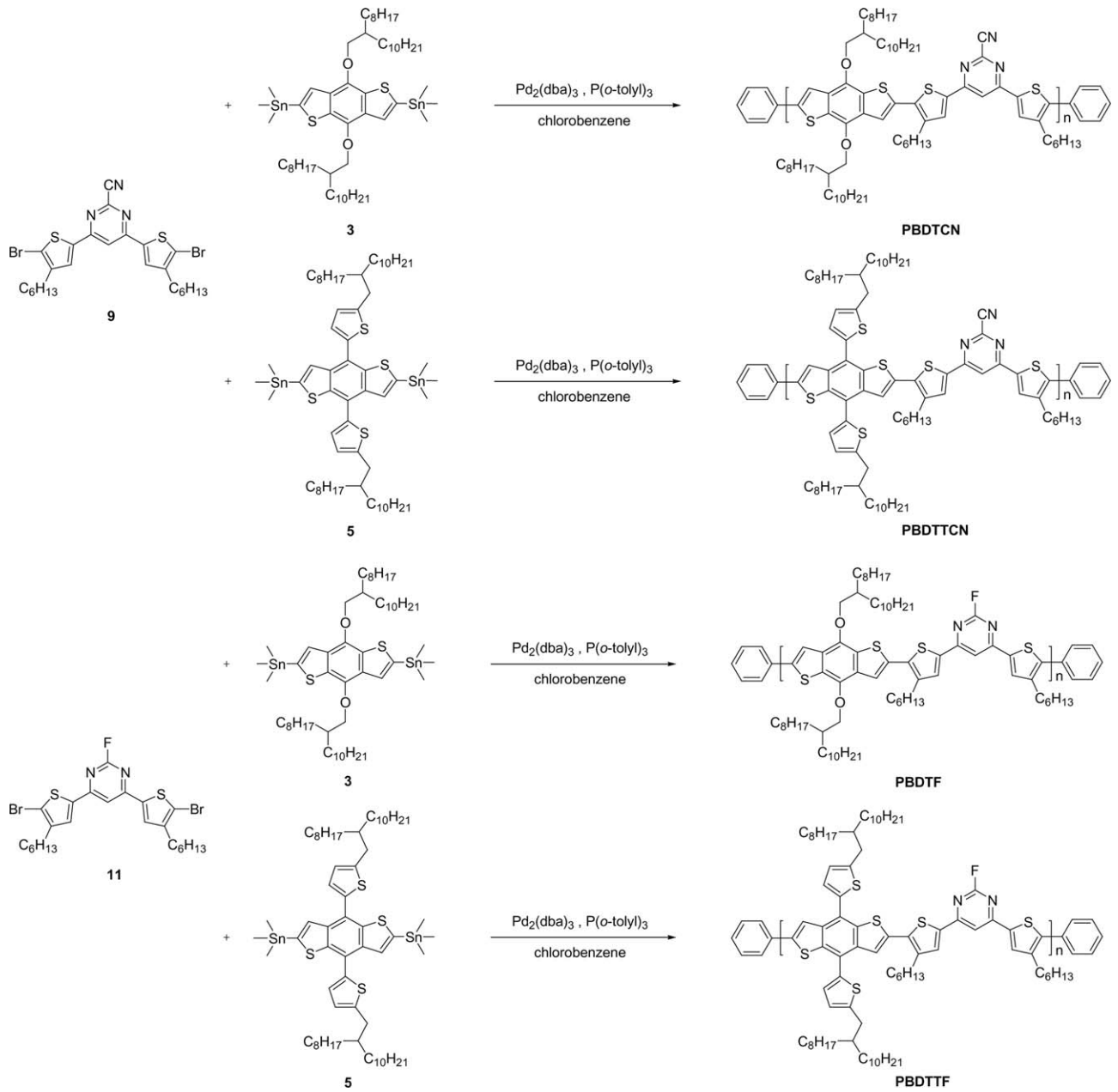

SCHEME 2 Synthetic route for the syntheses of the polymers.

fabrication of the polymer solar cells with the configuration of ITO/PEDOT:PSS/polymer:$PC_{71}BM$/Al.

EXPERIMENTAL

Instrumental Characterization

All reagents were purchased from Aldrich or TCI, and used without further purification. Solvents were purified by normal procedure and handled under moisture-free atmosphere. ^{1}H and ^{13}C NMR spectra were recorded with a Varian Gemini-300 (300 MHz) spectrometer and chemical shifts were recorded in ppm units with TMS as the internal standard. Flash column chromatography was performed with Merck silica gel 60 (particle size 230–400 mesh ASTM) with ethyl acetate/hexane or methanol/methylene chloride gradients unless otherwise indicated. Analytical thin layer chromatography (TLC) was conducted using Merck 0.25 mm silica gel 60F precoated aluminum plates with fluorescent indicator UV254. High resolution mass spectra (HRMS) were recorded on a JEOL JMS-700 mass spectrometer under electron impact (EI) conditions in the Korea Basic Science Institute (Daegu). Molecular weight and polydispersity of the polymer were determined by gel permeation chromatography (GPC) analysis with a polystyrene standard calibration and carried out at 35 °C. The differential scanning calorimetry (DSC) analysis was performed on a DSC Q200 at heating

TABLE 1 Polymerization Results and Thermal Properties of Polymers

Polymer	M_n[a]	M_w[a]	PDI[a]	DSC (T_g)	TGA (T_d)[b]
PBDTCN	20,000	60,000	3.00	101	324
PBDTTCN	38,000	220,000	5.70	99	410
PBDTF	10,000	26,000	2.54	102	329
PBDTTF	52,000	260,000	4.93	101	429

[a] Molecular weight (M_w) and polydispersity (PDI) of the polymers were determined by gel permeation chromatography (GPC) in $CHCl_3$ using polystyrene standards.
[b] Onset decomposition temperature (5% weight loss) measured by TGA under N_2.

rates of 10 °C/min. The thermal gravimetric analysis (TGA) was performed with a SDT Q600 under nitrogen atmosphere at a heating rate of 10 °C/min to 800 °C in the Korea Basic Science Institute (Busan). The UV-Vis absorption spectra were recorded by a Varian 5E UV/VIS/NIR spectrophotometer. Cyclic voltammogram of the polymers was obtained using an Wona-WPG100 at room temperature in a three-electrode cell under a Ar atmosphere at a scan rate of 100 mV/s, with Pt wire as the counter electrode, an $Ag/AgNO_3$ reference electrode, and 0.1 M tetraethylammonium tetrafluoroborate ($TBABF_4$) in acetonitrile as the electrolyte. The AFM instrumentation consisted of a Veeco NanoScope AFM and standard silicon cantilever (Veeco; tip radius, 8 nm; normal spring constant, 21–78 N/m; scan rate, 2.0 Hz) at ambient conditions (in air, 20 °C). GIWAXS were measured at the 5 Å beamline in the Pohang Accelerator Laboratory (PAL, South Korea). 2D GIWAXS patterns were recorded using CCD detector positioned at the end of a vacuum guide tube in which the X-ray pass through the thin films under vacuum, where operation conditions were set to a X-ray wavelength of 1.07153 Å and a sample-to-detector distance (SDD) of 482.08 mm. The incidence angle (0.1) was carefully chosen to allow for complete X-ray penetration of the film. The scattering spectra were collected as a two-dimensional image map oriented along the plane of the substrate (q_y) and the plane perpendicular to the substrate (q_z).

Device Fabrication and Measurements

The FETs were fabricated on heavily doped *n*-type silicon (Si) wafers each covered with a thermally grown silicon dioxide (SiO_2) layer with thickness of 200 nm. Whole Si substrates were cleaned with ultrasonic bath in acetone and isopropyl alcohol successively, dried over 2 h in the dry oven at 100 °C, and then subjected to UV-ozone treatment for 30 min. The active layer was deposited by spin coating at 2000 rpm. Before active layer deposition, SiO_2 surfaces were treated with octadecyltrichlorosilane (OTS) to make surface hydrophobic. All solutions were of 10 mg/mL concentration in chlorobenzene. The thickness of the deposited films was about 60 nm. Before deposition of source drain electrodes, the films were dried at room temperature for 30 min. Source and drain electrodes using Au were deposited by thermal evaporation using shadow mask. The thickness of source and drain electrodes was 50 nm. Channel length (L) and channel width (W) were 50 μm and 3.0 mm, respectively. Electrical characterization was performed using a Keithley semiconductor parametric analyzer (Keithley 4200). All fabrication and measurement processes were carried out in the glove box filled with N_2. The mobility (μ) was determined using the following equation in the saturation regime by

$$I_{sat} = (\mu W C_i / 2L) \cdot (V_{GS} - V_T)^2$$

where C_i is the capacitance per unit area of 15 nF cm^{-2} and V_T is the threshold voltage.

Solar cells were fabricated on an indium tin oxide (ITO)-coated glass substrate with the following structure; ITO-coated glass substrate/poly(3,4-ethylenedioxythiophene) polystyrene sulfonate (PEDOT:PSS)/polymer:$PC_{71}BM$/Al. The ITO-coated glass substrate was first cleaned with detergent, ultrasonicated in acetone and isopropyl alcohol, and subsequently dried overnight in an oven. PEDOT:PSS (Baytron PH) was spin-cast from aqueous solution to form a film of 40 nm thickness. The substrate was dried for 10 min at 140 °C in

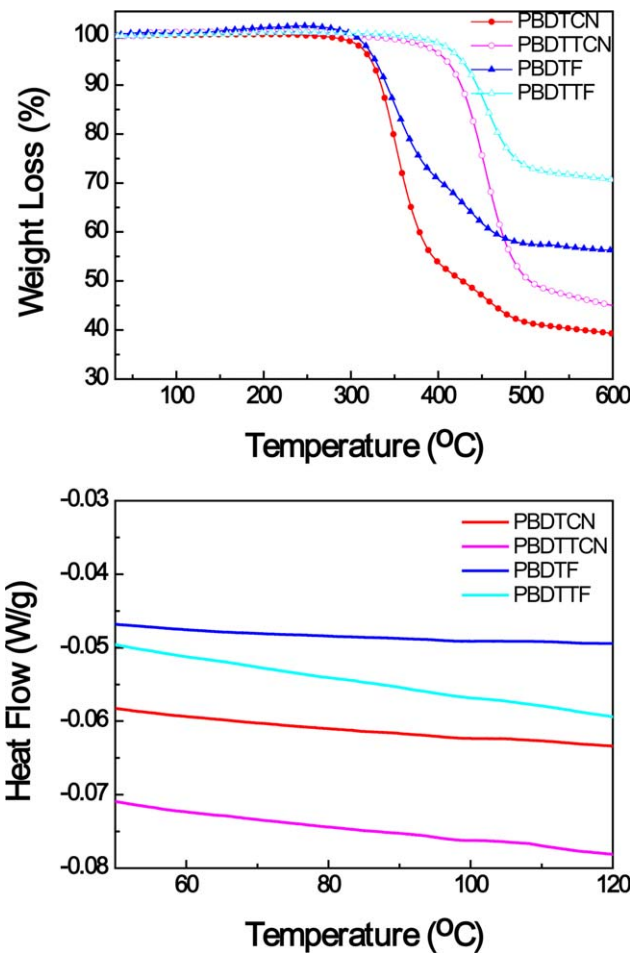

FIGURE 2 Thermogravimetric analysis of polymers under N_2. Inner: differential scanning calorimetry of polymers under N_2. [Color figure can be viewed in the online issue, which is available at wileyonlinelibrary.com.]

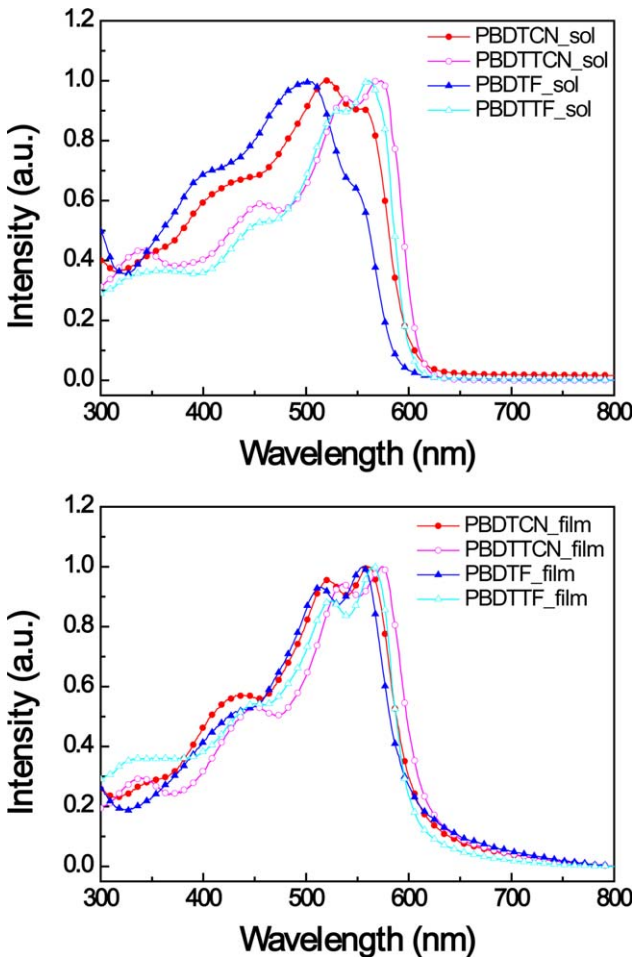

FIGURE 3 UV-Visible absorption spectra of polymers in chloroform solution and the solid state. [Color figure can be viewed in the online issue, which is available at wileyonlinelibrary.com.]

air and then transferred into a glove box to spin-cast the active layer. A solution containing a mixture of polymer:$PC_{71}BM$ in chlorobenzene solvent with concentration of 20 mg/mL was then spin-cast on top of the PEDOT:PSS layer. The film was dried for 30 min at room temperature in the glove box. Then, an aluminum (Al, 100 nm) electrode was deposited by thermal evaporation in a vacuum of about 3×10^{-6} Torr. Current density-voltage (*J–V*) characteristics of the devices were measured using a Keithley 2400 Source Measure Unit. Solar cell performance utilized an Air Mass 1.5 Global (AM 1.5 G) solar simulator with an irradiation

TABLE 2 Characteristics of the UV-Vis Absorption Spectra

Polymer	In solution	In thin film
PBDTCN	427, 520, 554	437, 521, 561
PBDTTCN	336, 453, 535, 569	337, 450, 536, 575
PBDTF	405, 500, 548	437, 513, 555
PBDTTF	336, 451, 526, 559	337, 445, 525, 565

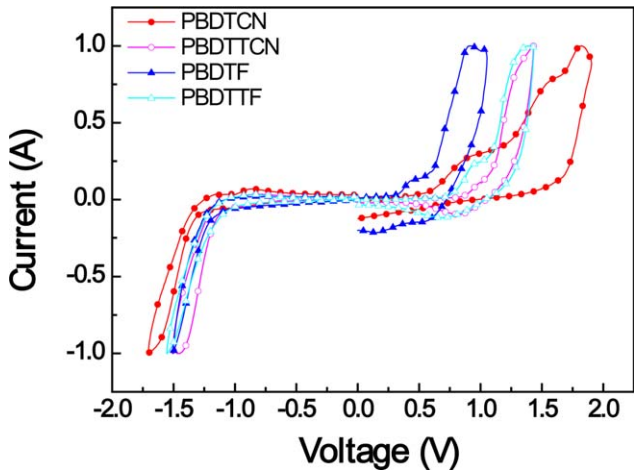

FIGURE 4 Cyclic voltammetry curves of the polymers in 0.1 M TBAF in acetonitrile solution at a scan rate of 100 mV/s at room temperature (vs. an Ag quasi-reference electrode). [Color figure can be viewed in the online issue, which is available at wileyonlinelibrary.com.]

intensity of 1000 W m^{-2}. The spectral mismatch factor was calculated by comparison of solar simulator spectrum with AM 1.5 spectrum at room temperature.

Synthesis of Monomers and Polymers

Synthesis of 4,8-Bis(2-Octyldodecyloxy)Benzo[1,2-B:3,4-B′]Dithiophene (2)

To the solution of benzo[1,2-*b*:4,5-*b*′]dithiophene-4,8-dion (**1**) (4.0 g, 18.0 mmol) and zinc powder (2.6 g, 40.0 mmol) in EtOH (16 mL) and DMF (16 mL), was added 5 N NaOH aqueous solution (25 mL) and the mixture was stirred under reflux for 3 h. After 1-iode-2-octyldodecane (22.3 g, 54.0 mmol) and tetrabutylammoniumbromide (0.9 g, 3.6 mmol) were added to the mixture at room temperature, the reaction mixture was refluxed for 12 h. The reaction mixture was then extracted with ethyl acetate, and the organic layer was washed with water and dried over anhydrous $MgSO_4$. After removing the solvent under reduced pressure, the residue was purified by flash to give 4.9 g (35%) of compound **2** as a colorless oil.

^{1}H NMR (300 MHz, $CDCl_3$) δ (ppm) 7.48 (d, 2H, J= 5.5 Hz), 7.36 (d, 2H, J = 5.5 Hz), 4.17 (d, 4H, J = 4.7 Hz), 1.92–1.80 (m, 2H), 1.72–1.60 (m, 4H), 1.53-1.20 (m, 60H), 0.90–0.87 (t, 12H, J = 6.9 Hz); ^{13}C NMR (75 MHz, $CDCl_3$) δ (ppm) 144.9, 131.7, 130.2, 126.1, 120.5, 39.4, 32.2, 31.6, 30.3, 30.1, 30.0, 29.9, 29.6, 27.2, 22.9, 14.4; HRMS (FAB^+, *m/z*) calcd. for $C_{50}H_{86}O_2S_2$ 783.6148, found 783.6158.

Synthesis of 2,6-Bis(Trimethyltin)-4,8-Bis(2-Octyldodecyloxy)Benzo[1,2-B:3,4-B′]Dithiophene (3)

To a solution of compound **2** (4.0 g, 5.1 mmol) in anhydrous THF (35 mL), was added dropwise *n*-butyllithium (2.5 M in hexane) (8.2 mL, 20.4 mmol) via syringe at −78 °C under argon atmosphere. The mixture was stirred at −78 °C for 30 min and then at room temperature for 30 min. After the mixture was

TABLE 3 Electrochemical Potentials and Energy Levels of the Polymers

Polymers	Optical band gap[a] (eV)	HOMO[b] (eV)	LUMO[c] (eV)	E_{ox}[d] (V)	E_{red}[d] (V)
PBDTCN	2.04	−5.39	−3.35	0.59	−1.34
PBDTTCN	2.01	−5.67	−3.66	0.87	−1.15
PBDTF	2.07	−5.14	−3.07	0.34	−1.22
PBDTTF	2.06	−5.58	−3.52	0.78	−1.18

[a] Optical energy band gap was estimated from the onset wavelength of the optical absorption.
[b] Calculated from the oxidation potentials.
[c] Estimated by HOMO + E_g^{opt}.
[d] Onset oxidation and reduction potential measured by cyclic voltammetry.

cooled to −78 °C again, trimethyltin chloride (1 M in THF) (25.5 g, 25.5 mmol) was added. The mixture was warmed to room temperature and stirred for 12 h. After quenching the reaction with water, the volatile species were evaporated under reduced pressure. The residue was extracted with diethyl ether, and the organic layer was washed with water, dried over anhydrous MgSO4, and concentrated. Recrystallization afforded 5.0 g (88%) of compound **3** as a colorless crystals; mp 38.5 °C.

^{1}H NMR (300 MHz, $CDCl_3$) δ (ppm) 7.51 (s, 2H), 4.17 (d, 4H, $J = 4.9$ Hz), 1.91–1.80 (m, 2H), 1.70–1.60 (m, 4H), 1.52–1.26 (m, 60H), 0.94–0.54 (t, 12H, $J = 7.1$ Hz), 0.45 (s, 18H); ^{13}C NMR (75 MHz, CDCl3) δ (ppm) 143.5, 140.6, 134.1, 133.1, 128.2, 39.4, 32.2, 31.6, 30.4, 30.1, 30.0, 29.9, 29.7, 29.6, 27.3, 22.9, 14.4, -8.1; HRMS (FAB^+, *m/z*) calcd. for C56H102O2S2Sn2 1110.5374, found 1110.5370.

Synthesis of 4,8-Bis(5-octyldodecylthiophen-2-Yl)Benzo[1,2-B;4,5-B′]Dithiophene (4)

In a dried three-neck 250 mL argon purged flask, *n*-butyllithium (2.5 M in hexane) (10.9 mL, 27.2 mmol) was added dropwise (30 min) to a mixture of 2-octyldodecylthiophene

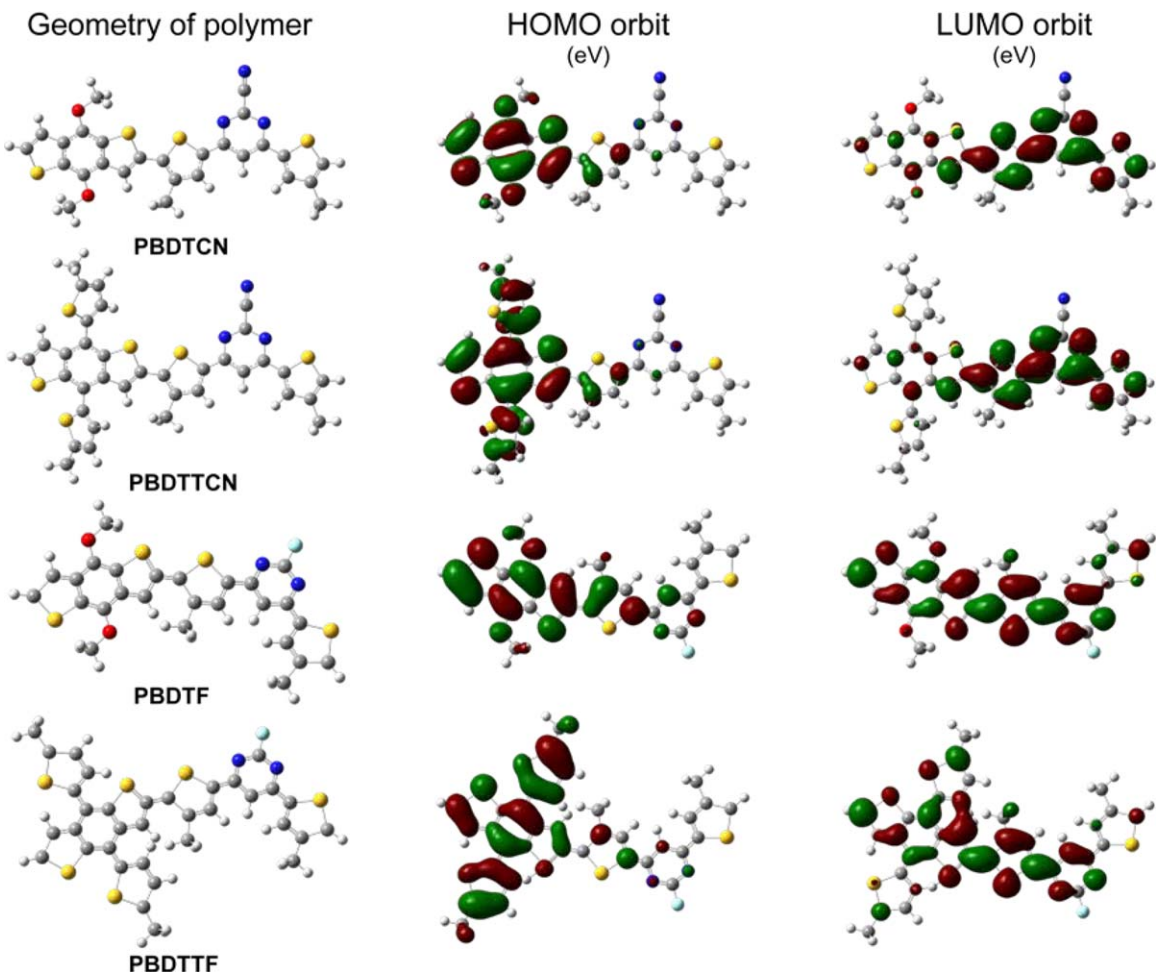

FIGURE 5 Optimized geometries and molecular orbital surfaces of the HOMO and LUMO of polymers at the B3LYP/6-311+G level of theory. [Color figure can be viewed in the online issue, which is available at wileyonlinelibrary.com.]

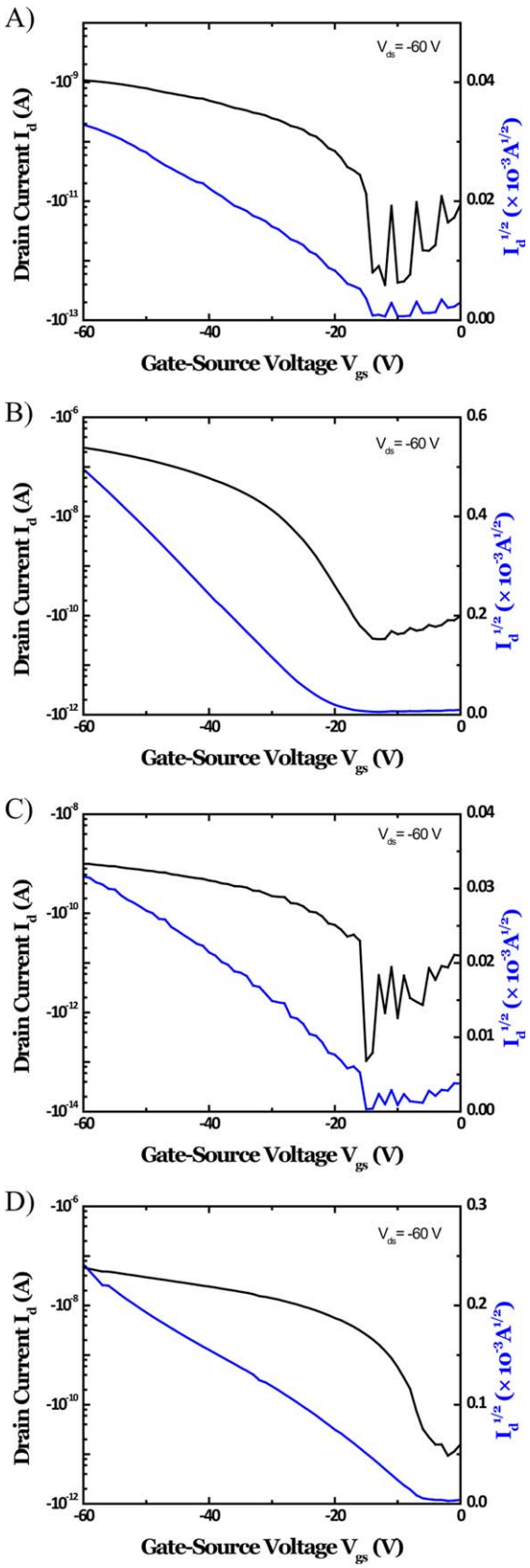

FIGURE 6 The OFET of polymers. [Color figure can be viewed in the online issue, which is available at wileyonlinelibrary.com.]

TABLE 4 OFET Characteristics of Polymers

Polymers	Mobility ($cm^2\ V^{-1}\ s^{-1}$)	I_{on}/I_{off}	V_{th} (V)
PBDTCN	1.64×10^{-6}	10^3 (2.8×10^3)	−10
PBDTTCN	4.06×10^{-4}	10^4 (7.3×10^3)	−22
PBDTF	1.07×10^{-6}	10^4 (9.6×10^3)	−8.4
PBDTTF	6.60×10^{-5}	10^4 (6.2×10^3)	−5.5

The OFETs are in bottom-gate, top-contact configuration with channel width (W) of 3 mm, and channel length (L) of 50 μm.

(6.0 g, 18.2 mmol) in 40 mL THF at 0 °C. The mixture was then warmed to 50 °C and stirred for 2 h, after that 4,8-dehydrobenzo[l,2-*b*:4,5-*b*′]dithiophene-4,8-dione (**1**) (2.0 g, 9.1 mmol) was subsequently added to the reaction mixture followed by stirring for 1.5 h at 50 °C. After cooling the reaction mixture to ambient temperature, $SnCl_2 2H_2O$ (15.4 g, 68.1 mmol) in 30 mL HCl (10%) was added and the mixture was stirred for additional 2 h, after which it was subsequently poured into ice water and extracted with diethyl ether. The combined organic layer was dried with anhydrous MgSO4. After removing the solvent under reduced pressure, the residue was purified by flash to give 5.0 g (30%) of compound **4** as a yellow oil.

^{1}H NMR (300 MHz, $CDCl_3$) δ (ppm) 7.65 (d, 2H, $J = 5.9$ Hz), 7.45 (d, 2H, $J = 5.9$ Hz), 7.29 (d, 2H, $J = 3.6$ Hz), 6.89 (d, 2H, $J = 3.6$ Hz), 2.86 (d, 4H, $J = 6.5$ Hz), 1.78–1.72 (m, 2H), 1.36–1.22 (m, 64H), 0.89 (t, 12H, $J = 7.0$ Hz); ^{13}C NMR (75 MHz, $CDCl_3$) δ (ppm) 146.0, 139.3, 137.5, 136.8, 127.9, 127.6, 125.6, 124.3, 123.7, 40.3, 34.9, 33.6, 32.2, 30.2, 29.9, 29.6, 26.9, 22.9, 14.3; HRMS (FAB^+, *m/z*) calcd. for $C_{58}H_{91}S_4$ 915.6004, found 915.6007.

Synthesis of 2,6-Bis(Trimethyltin)-4,8-Bis(5-octyldodecylthiophen-2-Yl)Benzo[1,2-B:4,5-B′]Dithiophene (5)

In a dry two-neck 50 mL argon purged flask, compound **4** (1.5 g, 1.4 mmol) was dissolved in 20 mL anhydrous THF. The solution was cooled to 0 °C and a solution of *n*-butyllithium (2.50 M in hexane) (1.5 mL, 3.8 mmol) was added dropwise with stirring. The reaction mixture was then stirred for 2 h at room temperature. Next, the reaction mixture was cooled to 0 °C and a Me_3SnCl solution (1 M in THF) (5.5 mL, 5.5 mmol) was added in one portion. The reaction mixture was stirred at 0 °C for 30 min and then warmed to room temperature. After stirring for 2 h, the reaction mixture was quenched by the addition of 10 mL distilled water, and extracted by diethyl ether. The combined organic phase was dried with anhydrous MgSO4 and concentrated to obtain yellow viscous crude product. Recrystallization afforded 1.0 g (74%) of compound **5** as light-yellow oil.

^{1}H NMR (300 MHz, $CDCl_3$) δ (ppm) 7.69 (s, 2H), 7.32 (d, 2H, $J = 3.5$ Hz), 6.90 (d, 2H, $J = 3.6$ Hz), 2.87 (d, 4H, $J = 6.5$ Hz), 1.80–1.70 (m, 2H), 1.40–1.22 (m, 64H), 0.88 (t, 12H, $J = 7.0$ Hz), 0.40 (s, 18H); ^{13}C NMR (75 MHz, $CDCl_3$) δ (ppm) 145.6,

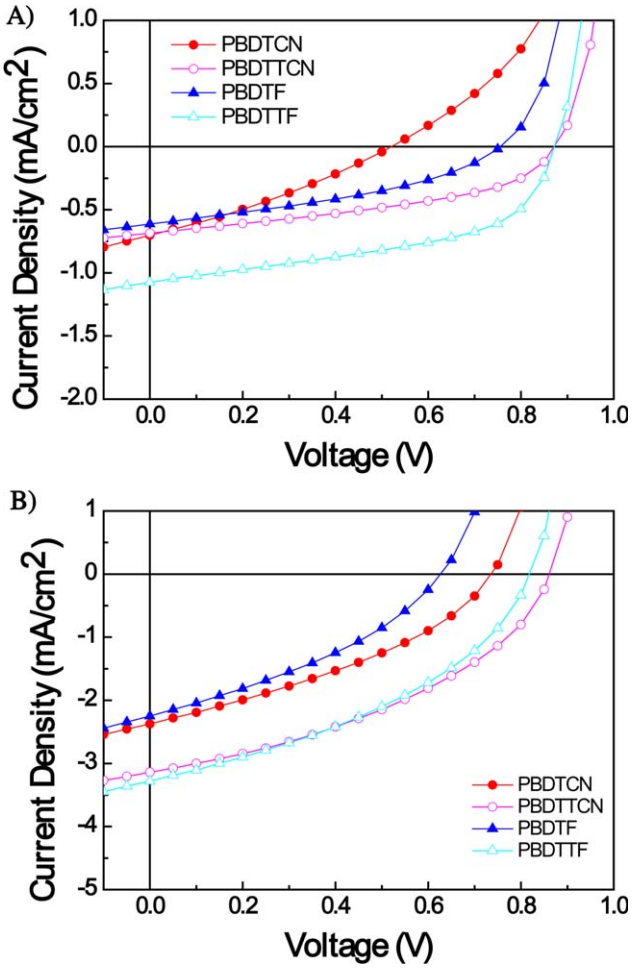

FIGURE 7 Current density-potential characteristics of the polymers solar cells under the illumination of AM 1.5, 100 mW/cm^2. A) Current density–voltage (*J*–*V*) of polymer:$PC_{71}BM$ blends without DIO, B) current density–voltage (*J*–*V*) of polymer:$PC_{71}BM$ blends with 3% DIO. [Color figure can be viewed in the online issue, which is available at wileyonlinelibrary.com.]

143.5, 142.4, 138.2, 138.0, 131.4, 127.8, 125.6, 122.7, 40.3, 34.9, 33.7, 32.2, 30.3, 30.0, 29.6, 27.0, 23.0, 14.4, −8.1; HRMS (FAB$^+$, *m/z*) calcd. for $C_{64}H_{106}S_4Sn_2$ 1242.5221, found 1242.5226.

Synthesis of 2-Chloro-4,6-Bis(4-hexyl-2-Thienyl) Pyrimidine (7)

To a stirred solution of 2,4,6-trichloropyrimidine (10.0 g, 54.5 mmol) and (4-hexyl-2-thienyl)(tributyl)stannane (**6**) (38.4 g, 114.5 mmol) in 30 mL of THF at room temperature was added dichloro*bis*(triphenylphosphine)palladium(II) (2 mol %). The reaction mixture was stirred for 24 h at 80 °C. After cooling room temperature, the reaction mixture was concentrated under reduced pressure, and purified by flash column chromatography to give 10.0 g (20%) of compound **7** as yellow oil.

^{1}H NMR (300 MHz, $CDCl_3$) δ (ppm) 7.73 (s, 2H), 7.57 (s, 1H), 7.18 (s, 2H), 2.65 (t, 4H, $J = 7.6$ Hz), 1.67 (qi, 4H, $J = 7.6$ Hz), 1.45–1.33 (m, 12H), 0.90 (t, 6H, $J = 6.5$ Hz); ^{13}C NMR (75 MHz, $CDCl_3$) δ (ppm) 161.8, 145.0, 140.1, 129.9, 126.1, 120.3, 107.1, 31.7, 30.5, 30.4, 28.9, 22.6, 14.1; HRMS(EI$^+$, *m/z*) calcd for $C_{24}H_{31}ClN_2S_2$ 446.1617, found 446.1617.

Synthesis of 4,6-Bis(4-hexyl-2-Thienyl)-2-Pyrimidinecarbonitrile (8)

To a stirred solution of 2-chloro-4,6-*bis*(4-hexyl-2-thienyl)-pyrimidine (**7**) (1.6 g, 3.6 mmol) in 20 mL of THF at RT under argon was added dropwise NaCN (0.8 g, 16.8 mmol) solution in TMA/H_2O (1:3). After stirring for 24 h, the reaction mixture was treated with 200 mL of water and 200 mL of diethyl ether. The aqueous phase was extracted with diethyl ether and combined organic layer was dried over $MgSO_4$. After removing the solvent under reduced pressure, the residue was purified by flash to give 1 g (60%) of compound **8** as a yellow oil.

^{1}H NMR (300 MHz, $CDCl_3$) δ (ppm) 7.75 (s, 2H), 7.73 (s, 1H), 7.23 (s, 2H), 2.66 (t, 4H, $J = 6.3$ Hz), 1.67 (qi, 4H, $J = 6.4$ Hz), 1.46-1.34 (m, 12H), 0.91 (t, 6H, $J = 6.5$ Hz); ^{13}C NMR (75 MHz, $CDCl_3$) δ (ppm) 160.3, 155.7, 145.3, 139.6, 130.2, 126.9, 115.8, 110.1, 31.6, 30.5, 30.4, 28.9, 22.6, 14.1; HRMS(EI$^+$, *m/z*) calcd. for $C_{25}H_{31}N_3S_2$ 437.1959, found 437.1962.

Synthesis of 4,6-Bis(5-bromo-4-hexyl-2-Thienyl)-2-Pyrimidinecarbonitrile (9)

To a stirred solution of 4,6-*bis*(4-hexyl-2-thienyl)-2-pyrimidinecarbonitrile (**8**) (0.5 g, 1.2 mmol) in DMF at 80 °C was added *N*-bromosuccinimide (NBS) (1.2 g, 6.9 mmol). After stirring over 6 h at 80 °C, 100 mL of water, and 100 mL of CH_2Cl_2 were added. The organic phase was washed with 3 × 100 mL of water. The organic phase was concentrated under reduced pressure and purified by flash column chromatography to give 0.5 g (73%) of compound **9** as yellow solid; mp 150 °C.

^{1}H NMR (300 MHz, $CDCl_3$) δ (ppm) 7.61 (s, 2H), 2.61 (t, 4H, $J = 7.6$ Hz), 1.65 (qi, 4H, $J = 7.6$ Hz), 1.47–1.35 (m, 12H), 0.91 (t, 6H, $J = 6.5$ Hz); ^{13}C NMR (75 MHz, $CDCl_3$) δ (ppm)

TABLE 5 Photovoltaic Properties of Polymers

Donor	3% DIO	V_{OC} (V)	J_{SC} (mA/cm^2)	FF	PCE (%)
PBDTCN	Without	0.52	0.70	0.30	0.11
	With	0.74	2.37	0.36	0.63
PBDTTCN	Without	0.87	0.68	0.44	0.26
	With	0.86	3.14	0.40	1.09
PBDTF	Without	0.76	0.61	0.38	0.17
	With	0.64	2.25	0.35	0.50
PBDTTF	Without	0.87	1.08	0.50	0.47
	With	0.82	3.28	0.39	1.05

Polymer:acceptor(1:1.5) 20 mg/mL in CB.

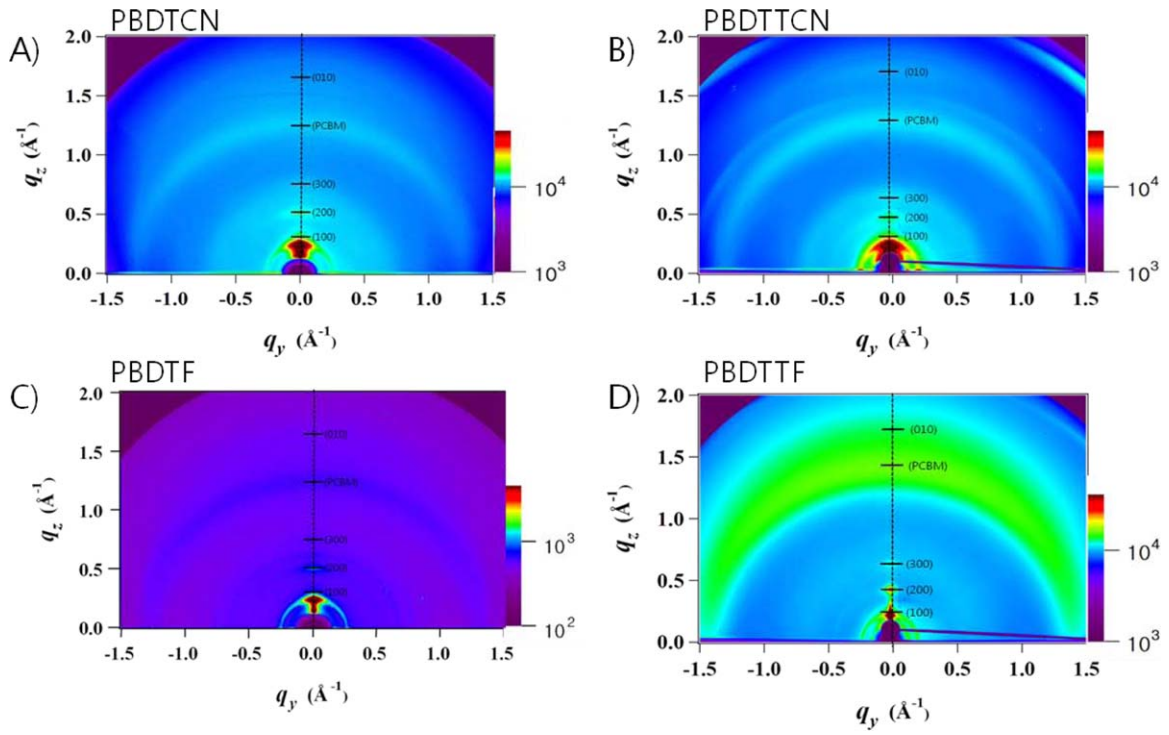

FIGURE 8 The GIWAX data of **PBDTCN**, **PBDTTCN**, **PBDTF**, or **PBDTTF**/$PC_{71}BM$ blend films. A) 2D patterns of **PBDTCN**, B) 2D patterns of **PBDTTCN**, C) 2D patterns of **PBDTF**, D) 2D patterns of **PBDTTF**. [Color figure can be viewed in the online issue, which is available at wileyonlinelibrary.com.]

159.4, 145.1, 144.4, 139.1, 129.6, 117.5, 115.5, 108.9, 31.6, 29.7, 29.6, 28.9, 22.6, 14.1; HRMS(FAB^+, *m/z*) calcd. for $C_{25}H_{30}N_3Br_2S_2$ 594.0248, found 594.0246.

Synthesis of 2-fluoro-4,6-Bis(4-hexyl-2-Thienyl) Pyrimidine (10)

A solution of 2-chloro-4,6-*bis*(4-hexyl-2-thienyl)pyrimidine (**7**) (3.0 g, 6.7 mmol), KF (2.0 g, 33.6 mmol), DCH-18-crown-6 (0.15 g, 0.4 mmol), and tetraglyme (14 mL) was heated at 150 °C overnight. After cooling to room temperature, the reaction mixture was treated with water and CH_2Cl_2. The aqueous phase was extracted with ethyl acetate and combined organic layer was dried with $MgSO_4$. After concentration of the organic phase under reduced pressure, the residue was purified by column chromatography to give 0.5 g (28%) of compound **10** as yellow oil.

^{1}H NMR (300 MHz, $CDCl_3$) δ (ppm) 7.75 (s, 2H), 7.60 (d, 1H, $J = 4.2$ Hz), 7.19 (s, 2H), 2.66 (t, 4H, $J = 7.7$ Hz), 1.67 (qi, 4H, $J = 7.6$ Hz), 1.48–1.34 (m, 12H), 0.91 (t, 6H, $J = 6.5$ Hz); ^{13}C NMR (75 MHz, $CDCl_3$) δ (ppm) 163.4, 145.0, 140.2, 130.0, 126.2, 106.6, 106.5, 31.6, 30.5, 30.4, 28.9, 22.6, 14.1; HRMS(EI^+, *m/z*) calcd. for $C_{24}H_{31}FN_2S_2$ 430.1913, found 430.1916.

Synthesis of 4,6-Bis(5-bromo-4-hexyl-2-Thienyl)-2-Fluoropyrimidine (11)

To a stirred solution of 2-fluoro-4,6-*bis*(4-hexyl-2-thienyl)-pyrimidine (**10**) (0.5 g, 1.1 mmol) in DMF at 80 °C was added *N*-bromosuccinimide (NBS) (1.2 g, 6.4 mmol). After 6 h at 80 °C, water and CH_2Cl_2 were added. The organic phase was washed with 3 × 100 mL of water. The organic phase was concentrated under reduced pressure and purified by flash column chromatography to give 0.2 g (20%) of compound **11** as yellow solid, m.p. 97 °C.

^{1}H NMR (300 MHz, $CDCl_3$): δ (ppm) 7.11 (s, 2H), 2.73 (t, 4H, $J = 7.6$ Hz), 1.76 (qi, 4H, $J = 7.6$ Hz), 1.45–1.30 (m, 12H), 0.90 (t, 6H, $J = 7.0$ Hz); ^{13}C NMR (75 MHz, $CDCl_3$) δ (ppm) 207.1, 164. 5, 162.4 (d, $^2J_{C\text{-}F} = 12.7$ Hz), 141.9 (d, $^1J_{C\text{-}F} = 338.6$ Hz), 129.4, 116.6, 105.5, 31.6, 29.7, 29.6, 28.9, 22.6, 14.1; HRMS(EI^+, *m/z*) calcd. for $C_{24}H_{29}Br_2FN_2S_2$ 586.0123, found 586.0120.

Synthesis of Poly(4,6-Bis(4-hexyl-2-Thienyl)-2-pyrimidinecarbonitrile-alt-4,8-Di(2-Octyldodecyloxy)Benzo[1,2-B;3,4-B′]Dithiophene) (PBDTCN)

Carefully purified 2,6-*bis*(trimethyltin)-4,8-*bis*(2-octyldodecyloxy)benzo[1,2-*b*:3,4-*b*′]dithiophene (**3**) (1 eq), 4,6-bis(5-bromo-4-hexyl-2-thienyl)-2-pyrimidinecarbonitrile (**9**) (1 eq), P(o-tolyl)$_3$ (0.4 eq) and $Pd_2(dba)_3$ (3 mol %) were dissolved in chlorobenzene. The reaction mixture was refluxed with vigorous stirring for 2 days under argon atmosphere. After cooling to room temperature, the reaction mixture was poured into methanol and 1 M HCl. The precipitated material was recovered by filtration. The resulting solid material was reprecipitated using 100 mL of chloroform/1.0 L of methanol several times to remove residual amount of the catalyst. The solid was washed for 2 days in a Soxhlet extractor using an

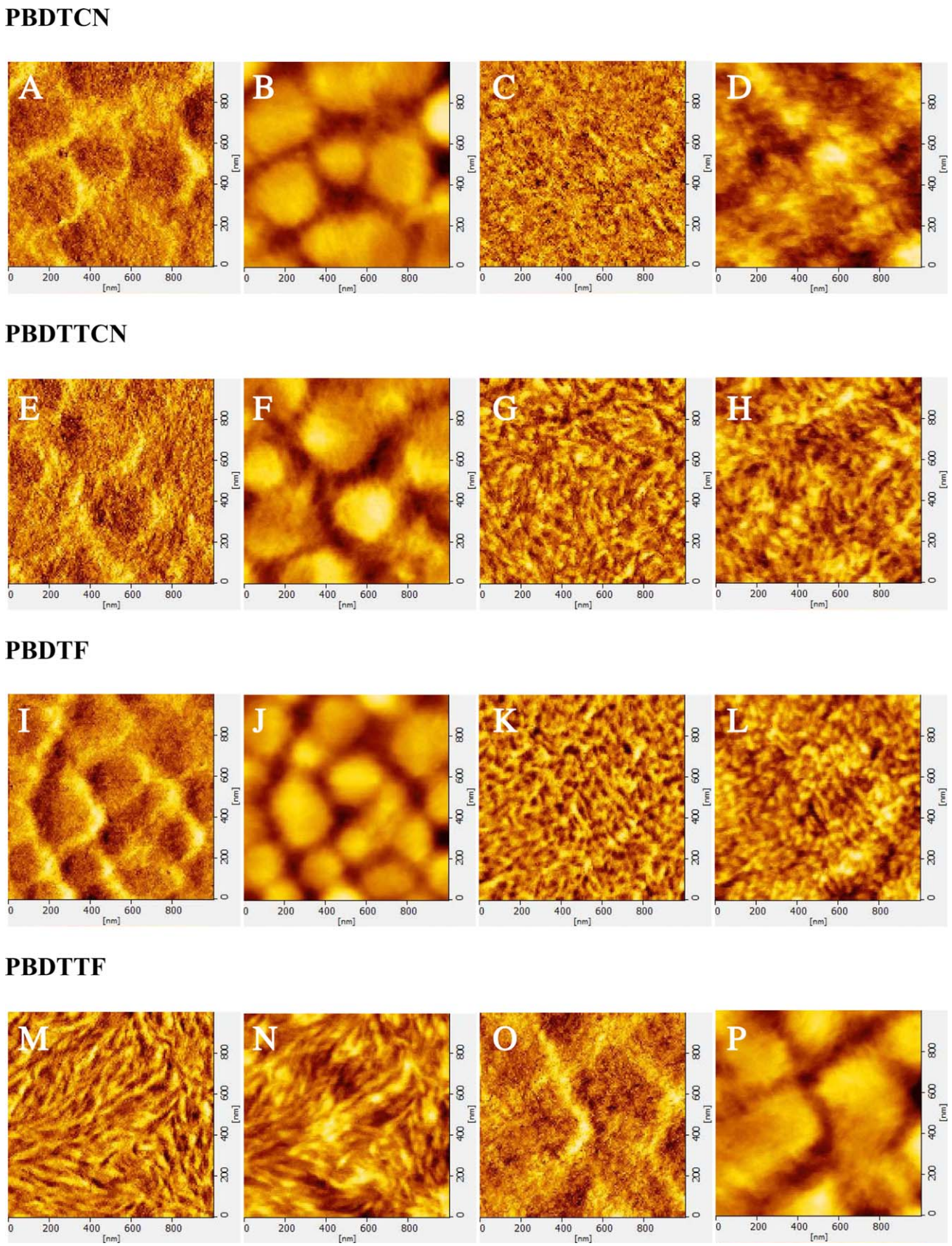

FIGURE 9 AFM phase images (A, C, E, G, I, K, M, and O) and topography (B, D, F, H, J, L, N, and P) of the polymer/PCBM (1:1.5, w/w) without DIO (A, E, I, and M) and with DIO (C, G, K, and O). (scan size: 1 μm $\times$ 1 μm). [Color figure can be viewed in the online issue, which is available at wileyonlinelibrary.com.]

acetone/methanol mixture to remove oligomers and catalyst residue. The solid was washed for two days in a Soxhlet extractor using an acetone/methanol mixture to remove oligomers and catalyst residue. The final product was obtained after drying under vacuum at 60 °C. The resulting polymer was soluble in THF, $CHCl_3$, ODCB, and toluene.

Synthesis of Poly(4,6-Bis(4-hexyl-2-Thienyl)-2-pyrimidinecarbonitrile-alt-4,8-Bis(5-(2-Octyldodecyloxy)Thiophen-2-Yl)Benzo[1,2-B:4,5-B′]Dithiophene) (PBDTTCN)

Carefully purified 2,6-*bis*(trimethyltin)-4,8-*bis*(5-octyldodecylthiophen-2-yl)benzo[1,2-*b*:4,5-*b′*]dithiophene (**5**) (1 eq), 4,6-*bis*(5-bromo-4-hexyl-2-thienyl)-2-pyrimidinecarbonitrile (**9**) (1 eq), P(o-tolyl)$_3$ (0.4 eq), and $Pd_2(dba)_3$ (3 mol %) were dissolved in chlorobenzene. The reaction mixture was refluxed with vigorous stirring for 2 days under argon atmosphere. After cooling to room temperature, the reaction mixture was poured into methanol and 1 M HCl. The precipitated material was recovered by filtration. The resulting solid material was reprecipitated using 100 mL of chloroform/1.0 L of methanol several times to remove residual amount of the catalyst. The solid was washed for 2 days in a Soxhlet extractor using an acetone/methanol mixture to remove oligomers and catalyst residue. The solid was washed for 2 days in a Soxhlet extractor using an acetone/methanol mixture to remove oligomers and catalyst residue. The final product was obtained after drying under vacuum at 60 °C. The resulting polymer was soluble in THF, $CHCl_3$, ODCB, and toluene.

Synthesis of Poly(4,6-Bis(4-hexyl-2-Thienyl)-2-fluoropyrimidine-alt-4,8-Di(2-Octyldodecyloxy)Benzo[1,2-B;3,4-B′]Dithiophene) (PBDTF)

Carefully purified 2,6-*bis*(trimethyltin)-4,8-*bis*(2-octyldodecyloxy)benzo[1,2-*b*:3,4-*b′*]dithiophene (**3**) (1 eq), 4,6-*bis*(5-bromo-4-hexyl-2-thienyl)-2-fluoropyrimidine (**11**) (1 eq), P(o-tolyl)$_3$ (0.4 eq), and $Pd_2(dba)_3$ (3 mol %) were dissolved in chlorobenzene. The reaction mixture was refluxed with vigorous stirring for 2 days under argon atmosphere. After cooling to room temperature, the reaction mixture was poured into methanol and 1 M HCl. The precipitated material was recovered by filtration. The resulting solid material was reprecipitated using 100 mL of chloroform/1.0 L of methanol several times to remove residual amount of the catalyst. The solid was washed for 2 days in a Soxhlet extractor using an acetone/methanol mixture to remove oligomers and catalyst residue. The solid was washed for 2 days in a Soxhlet extractor using an acetone/methanol mixture to remove oligomers and catalyst residue. The final product was obtained after drying under vacuum at 60 °C. The resulting polymer was soluble in THF, $CHCl_3$, ODCB, and toluene.

Synthesis of Poly(4,6-bis(4-hexyl-2-thienyl)-2-fluoropyrimidine-alt-4,8-bis(5-(2-octyldodecyloxy)thiophen-2-Yl)benzo[1,2-B:4,5-B′]dithiophene) (PBDTTF)

Carefully purified 2,6-*bis*(trimethyltin)-4,8-*bis*(5-octyldodecylthiophen-2-yl)benzo[1,2-*b*:4,5-*b′*]dithiophene (**5**) (1 eq), 4,6-*bis*(5-bromo-4-hexyl-2-thienyl)-2-fluoropyrimidine (**11**) (1 eq), P(o-tolyl)$_3$ (0.4 eq), and $Pd_2(dba)_3$ (3 mol %) were dissolved in chlorobenzene. The reaction mixture was refluxed with vigorous stirring for 2 days under argon atmosphere. After cooling to room temperature, the reaction mixture was poured into methanol and 1 M HCl. The precipitated material was recovered by filtration. The resulting solid material was reprecipitated using 100 mL of chloroform/1.0 L of methanol several times to remove residual amount of the catalyst. The solid was washed for 2 days in a Soxhlet extractor using an acetone/methanol mixture to remove oligomers and catalyst residue. The solid was washed for 2 days in a Soxhlet extractor using an acetone/methanol mixture to remove oligomers and catalyst residue. The final product was obtained after drying under vacuum at 60 °C. The resulting polymer was soluble in THF, $CHCl_3$, ODCB, and toluene.

RESULTS AND DISCUSSION

Synthesis and Characterization

The general synthetic routes toward the intermediates and polymers are outlined in Schemes 1 and 2. 2,6-*Bis*(trimethyltin)-4,8-*bis*(2-octyldodecyloxy)benzo[1,2-*b*:3,4-*b′*]dithiophene (**3**), which was prepared from benzo[1,2-*b*:4,5-*b′*]dithiophene-4,8-dione (**1**) over two steps, and 4,6-*bis*(5-bromo-4-hexyl-2-thienyl)-2-pyrimidinecarbonitrile (**9**), which was prepared from 2,4,6-trichloropyrimidine over three steps, were coupled to provide **PBDTCN** through Stille reaction with Pd(0)-catalyst. 2,6-*Bis*(trimethyltin)-4,8-*bis*(5-octyldodecylthiophen-2-yl)benzo[1,2-*b*:4,5-*b′*]dithiophene (**5**), which was prepared from compound **1** over two steps, and compound **9** were coupled to provide **PBDTTCN** through Stille reaction with Pd(0)-catalyst. By using the same polymerization condition, compound **3** and 4,6-*bis*(5-bromo-4-hexyl-2-thienyl)-2-fluoropyrimidine (**11**), which was prepared from 2,4,6-trichloropyrimidine over three steps, were coupled to provide **PBDTF** through Stille reaction with Pd(0)-catalyst. Compound **5** and compound **11** were coupled to provide **PBDTTF** through Stille reaction with Pd(0)-catalyst. All of the polymers show good solubility at room temperature in organic solvents such as chloroform, THF, chlorobenzene, and *o*-dichlorobenzene (ODCB).

Table 1 summarizes the polymerization results including molecular weights, PDI, and thermal stability of the copolymers. The number-average molecular weights (M_n) of 20,000, 38,000, 10,000, and 52,000 and weight-average molecular weights (M_w) of 60,000, 220,000, 26,000, and 260,000 with PDI (poly dispersity index, M_w/M_n) values of 3.0, 5.7, 2.5, and 4.5 were determined by gel permission chromatography (GPC) with a polystyrene standard in a chloroform eluent for the **PBDTCN**, **PBDTTCN**, **PBDTF,** and **PBDTTF**, respectively.

The thermal properties of the polymers were characterized by both DSC and TGA as shown in Figure 2 and summarized in Table 1. The polymers show good thermal stability with onset decomposition temperatures (T_d, 5% weight loss) of

324, 410, 329, and 429 °C, respectively. All polymers have glass transition temperature (T_g) values above 100 °C, thus they show thermal stability. **PBDTTCN** and **PBDTTF** with BDTT unit show especially higher thermal stability than the case of alkoxy-substituted BDT unit, which is attributed to the BDTT fragment with the more rigid structure.[16] The high thermal stability of the resulting polymers prevents the deformation of the morphology and is important for OPV device applications.

Optical Properties of the Polymers

The optical properties of solutions and films of the polymers were investigated by UV-Vis absorption spectroscopy. The solution was prepared using ODCB as a solvent and the thin film by spin-coating on quartz plates from the solution in ODCB. The UV-Vis absorption spectra of the polymers as solutions and thin films are shown in Figure 3 and summarized in Table 2. The solution of **PBDTCN** presents absorption bands with maximum peaks at 427, 520 and 554 nm. The **PBDTCN** thin film shows absorption band with peaks at 437, 521, and 561 nm and the absorption onset at 608 nm, corresponding to band gap of 2.04 eV. The maximum absorption peaks of **PBDTTCN** appear at about 336, 453, 535, and 569 nm in ODCB solution. The spectra of the **PBDTTCN** thin film shows absorption bands with maximum peaks at about 337, 450, 536, and 575 nm and the absorption onsets at 617 nm, corresponding to band gap of 2.01 eV. The maximum absorption peaks of **PBDTF** and **PBDTTF** appear at 405, 500, 548 nm and 336, 451, 526, 559 nm in ODCB solution, respectively. The maximum absorption peaks in solid thin films were at around 437, 513, 555 nm and 337, 445, 525, 565 nm, and the absorption onsets at 599, 602 nm, corresponding to band gap of 2.07, 2.06 eV, respectively. The short-wavelength absorption peaks have been ascribed to a delocalized excitonic π–π^* transition in the polymer chains and the long-wavelength absorption peaks attributed to the intramolecular charge transfer (ICT) between the substituted BDT/BDTT as electron rich unit and pyrimidine as electron deficient unit.[17] As shown in Figure 3, the absorption spectra of the **PBDTTCN** and **PBDTTF** films show red shifts of the long wavelength absorption peaks compared with the cases of **PBDTCN** and **PBDTF** due to the extended π-conjugation of the BDTT unit.[16,18] The red shift absorption demonstrates that the π–π stacking or interchain interaction of the polymers containing BDTT unit is better than those of the polymers with BDT unit. Similar trends were also reported for other BDT- and BDTT-based polymers.[16]

Electrochemical Properties of the Polymers

The CV was performed with a solution of tetrabutylammonium tetrafluoroborate (Bu_4NBF_4) (0.10 M) in acetonitrile at a scan rate of 100 mV/s at room temperature under argon atmosphere. A platinum electrode, Pt wire, and $Ag/AgNO_3$ electrode were used as the working, counter and reference electrode, respectively. The energy level of the $Ag/AgNO_3$ reference electrode (calibrated by the FC/FC^+ redox system) was 4.8 eV below the vacuum level. The cyclic voltammetry curves are shown in Figure 4 and the electrochemical data are summarized in Table 3. The energy levels of HOMO and lowest unoccupied molecular orbital (LUMO) were calculated according to the empirical formula of ($E_{HOMO} = -([E_{onset}]^{ox} + 4.8)$ eV) and ($E_{LUMO} = -(E_{HOMO} + E_g^{opt})$ eV), respectively.

The polymers, **PBDTCN**, **PBDTTCN**, **PBDTF,** and **PBDTTF**, exhibited the absorption onset wavelengths of 608, 617, 599, and 602 nm in solid thin film, which corresponds to band gaps of 2.04, 2.01, 2.07, and 2.06 eV, respectively. The polymers exhibit irreversible processes in an oxidation scan. The oxidation onsets of the polymers, **PBDTCN**, **PBDTTCN**, **PBDTF,** and **PBDTTF**, were estimated to be 0.59, 0.87, 0.34, and 0.78 V, which correspond to HOMO energy levels of −5.39, −5.67, −5.14, and −5.58 eV, respectively. When the alkoxy side chain was substituted with the alkylthiophene conjugated side chain, the HOMO and LUMO levels of the polymers are moved to lower energy values. The HOMO energy levels of **PBDTTCN** and **PBDTTF** are lower than those of **PBDTCN** and **PBDTF**.[19] Gadisa et al. have studied a relationship between the oxidation potential of polythiopene derivative and V_{OC} in BHJ type PSCs.[20] The V_{OC} depends on the oxidation potential of p-conjugated polymer as well.[21] The lower HOMO energy levels of the two-dimensional (2D) conjugated polymers, as in the case of BDTT series, could have higher V_{OC} values for the improvement of photovoltaic property and additional merit of improving oxidative stability.[22,23]

The optimized geometry and the HOMO and LUMO energy levels were calculated at the B3 LYP/6-31+G (d,p) level of theory using the Gaussian 03 package,[24] as shown in Figure 5. The HOMO and LUMO surfaces were plotted using the GaussView version 4.1. To simplify the calculation, the alkyl chains were replaced by methyl groups. For **PBDTCN** and **PBDTTCN**, the electron densities of the HOMOs is mainly distributed on the BDT unit (the electron rich unit), while those of the LUMOs on the pyrimidine unit (the electronic deficient unit), suggesting that the polymers are typical D–A types. For **PBDTF** and **PBDTTF**, the electron densities of the HOMOs show similar distribution mainly on the BDT unit (the electron rich unit), while those of the LUMOs is delocalized on the polymer backbone.[25,26]

Field-Effect Transistor and Photovoltaic Properties of the Polymers

The field-effect carrier mobilities of the polymers were measured by fabricating thin film field-effect transistors (FETs) using the top-contact geometry. Figure 6 shows the FET transfer characteristics of the polymer devices of the OTS-modified SiO_2 substrate. Hole mobilities of the polymers were calculated from the transfer characteristics of the OFETs and summarized in Table 4. The field-effect hole mobilities of **PBDTCN**, **PBDTTCN**, **PBDTF** and **PBDTTF** are 1.6×10^{-6}, 4.1×10^{-4}, 1.1×10^{-6}, and 6.6×10^{-5} cm^2/Vs, respectively. In case of the polymers with BDTT, the mobilities were increased caused by its better crystallinity.

The photovoltaic properties of the polymers were investigated by fabricating the OPVs with ITO as positive electrode,

the blend with polymers (**PBDTCN**, **PBDTTCN**, **PBDTF,** and **PBDTTF**) and $PC_{71}BM$ as active layer, and Al as negative electrode. Figure 7 shows the current-voltage (*I–V*) curves of the OPVs with the configuration of ITO/PEDOT:PSS/polymer:$PC_{71}BM$/Al under AM 1.5G irradiation (100 mW/cm^2) which are summarized in Table 5. The BHJ active layers were obtained by spin-coating of 2% (w/v) chlorobenzene solutions comprising a blend of polymers and $PC_{71}BM$ with or without diiodooctane (DIO) additive. The device with **PBDTTCN** and $PC_{71}BM$ with 3% DIO show a V_{OC} of 0.86 V, a J_{SC} of 3.14 mA/cm^2, and a fill factor (FF) of 0.40, giving a power conversion efficiency of 1.09%. The device comprising **PBDTTF** and $PC_{71}BM$ with 3% DIO show a V_{OC} of 0.82 V, a short circuit current density (J_{SC}) of 3.28 mA/cm^2, and a FF of 0.39, giving a power conversion efficiency of 1.05%. The **PBDTCN** and **PBDTF** device provided poor performance because of its more disordered structure. The enhanced efficiency of **PBDTTCN** and **PBDTTF** results from the good crystallinity with the extended π-conjugation caused by the BDTT unit. The better performance of **PBDTTF** and **PBDTTCN** is in good accordance with their higher hole-mobilities around 10^{-4} order as compared with the case of **PBDTF** and **PBDTCN**.

Two-Dimensional Grazing-Incidence Wide-Angle X-Ray Scattering (2D-GIWAXS) and Structural Properties of the Polymer

2D-GIWAX was measured to determine the extent of cofacial π-stacking, crystallinity, and the polymer-packing orientation relative to the substrate. Figure 8 shows the 2D-GIWAX images of **PBDTCN**, **PBDTTCN**, **PBDTF,** or **PBDTTF**:$PC_{71}BM$ blends with 3% DIO. In Figure 8(A,C), 2D-GIWAX image of **PBDTCN** or **PBDTF**: $PC_{71}BM$ blends with BDT unit shows weak diffraction peaks at $q_z = 0.27$ and 0.28 Å^{-1}, which correspond to the (100) reflection of the polymer crystal with a lamellar domain spacing (lattice parameter) of 2.37 and 2.29 nm. In Figure 8(B,D) of **PBDTTCN** or **PBDTTF**:$PC_{71}BM$ blends, very strong (100) peaks at around 0.26 and 0.27 Å^{-1} were observed, which correspond to a lattice parameter of 2.78 and 2.35 nm. Furthermore, the film with BDTT showed (100), (200), and (300) peaks with more pronounced reflections, indicating that the polymer stacks in the film have higher structural organization than the case with BDT. In both cases, a (010) $\pi-\pi$ stacking peaks at around 1.71 to 1.73 Å^{-1} were observed, which corresponds to a (010) of 0.36 nm. This is a typical $\pi-\pi$ stacking distance in conjugated polymers for high photovoltaic performances.[27,28] The fact that **PBDTTCN** or **PBDTTF**:$PC_{71}BM$ blends show large lattice parameter and higher intensity indicates their good crystallinity.[23]

Morphology of the Polymers

Atomic force microscopy (AFM) studies revealed the morphology of the blend films (polymer:$PC_{71}BM$ = 1:1.5 w/w) as shown in Figure 9, where the images were obtained in a surface area of 1.0 × 1.0 μm^2 by the tapping mode. The AFM image of **PBDTCN**, **PBDTTCN**, **PBDTF,** and **PBDTTF** without DIO exhibit root mean square (RMS) roughness of 6.07 nm, 4.39 nm, 8.70 nm, and 5.25 nm. In comparison, **PBDTCN**, **PBDTTCN**, **PBDTF** and **PBDTTF** with 3% DIO exhibit smaller RMS values of 2.61 nm, 1.85 nm, 1.95 nm, and 2.09 nm than the cases without DIO. The smoother surfaces, without large domains caused by the addition of the DIO additive, improves the interpenetrating network for optimal charge generation and transport. The higher hole mobility in addition to the improved morphology with 3% DIO is in good accordance with their higher values of J_{SC} and FF.[6]

CONCLUSIONS

PBDTCN, PBDTTCN, PBDTF, and **PBDTTF** with substituted-BDT/BDTT units as the electron rich units and pyrimidines, with cyano or fluoro groups, as the electron deficient units, were synthesized by Stille coupling reaction with Pd(0)-catalyst to provide good solubility in common organic solvents. The absorption spectra of **PBDTTCN** and **PBDTTF** thin films show shift to a longer wavelength region than **PBDTCN** and **PBDTF**. Solution-processed OPVs with the polymers as donor and $PC_{71}BM$ as the acceptor were fabricated, and the experimental conditions with different blending ratios and DIO additive were optimized. The device comprising **PBDTTCN** and $PC_{71}BM$ (1:1.5) with 3% DIO showed a V_{OC} of 0.86 V, a J_{SC} of 3.14 mA/cm^2, and a FF of 0.40, giving a power conversion efficiency of 1.09%. The device comprising **PBDTTF** and $PC_{71}BM$ (1:1.5) with 3% DIO showed a V_{OC} of 0.82 V, a J_{SC} of 3.28 mA/cm^2, and a fill factor (FF) of 0.39, giving a power conversion efficiency of 1.05%. **PBDTTCN** and **PBDTTF** provide the high V_{OC} values and the hole mobility of around 10^{-4} order and addition of DIO additive improved the morphology significantly, which is in good accordance with the device performances of the series. The 2D-GIWAX measurement revealed that **PBDTTCN** and **PBDTTF**:$PC_{71}BM$ blends with DIO have high structural organization.

ACKNOWLEDGMENT

This work was supported by the National Research Foundation of Korea (NRF) grant funded by the Korea Government (MEST) (NRF-2014R1A1A2055318).

REFERENCES AND NOTES

1 X. Wang, P. Jiang, Y. Chen, H. Luo, Z. Zhang, H. Wang, X. Li, G. Yu, Y. Li, *Macromolecules* **2013**, *46*, 4805–4812.

2 Y. Ma, Q. Zheng, Z. Yin, D. Cai, S. C. Chen, C. Tang, *Macromolecules* **2013**, *46*, 4813–4821.

3 L. Wang, D. Cai, Q. Zheng, C. Tang, S. C. Chen, Z. Yin, *ACS. Macro. Lett.* **2013**, *2*, 605–608.

4 N. Wang, Z. Chen, W. Wei, Z. Jiang, *J. Am. Chem. Soc.* **2013**, *135*, 17060–17068.

5 Y. Li, J. Zou, H. L. Yip, C. Z. Li, Y. Zhang, C. C. Chueh, J. Intemann, Y. Xu, P. W. Liang, Y. Chen, A. K. Y. Jen, *Macromolecules* **2013**, *46*, 5497–5503.

6 H. C. Chen, Y. H. Chen, C. C. Liu, Y. C. Chien, S. W. Chou, P. T. Chou, *Chem. Mater.* **2012**, *24*, 4766–4772.

7 F. Zhang, K. G. Jespersen, C. Bj€orstr €om, M. Svensson, M. R. Andersson, V. Sundstr€om, K. Magnusson, E. Moons, A. Yartsev, O. Ingan€as, *Adv. Funct. Mater.* **2006**, *16*, 667–674.

8 M. M. Wienk, M. Turbiez, J. Gilot, R. A. J. Janssen, *Adv. Mater.* **2008**, *20*, 2556–2560.

9 (a.) Y. Zou, A. Najari, P. Berrouard, S. Beaupr, E. B. Aïch, Y. Tao, M. A. Leclerc, Am. Chem. Soc. **2010**, *132*, 5330–5331; (b) C. Piliego, T. W. Holcombe, J. Douglas, C. H. Woo, P. M. Beaujuge, J. M. J. Frechet, J. Am. Chem. Soc. **2010**, *132*, 7595–7597.

10 T. Y. Chu, J. Lu, S. Beaupr, Y. Zhang, J. -R. Pouliot, S. Wakim, J. Zhou, M. Leclerc, Z. Li, J. Ding, Y. Tao, *J. Am. Chem. Soc.* **2011**, *133*, 4250–4253.

11 J. Huang, Y. Zhao, X. Ding, H. Jia, B. Jiang, Z. Zhang, C. Zhan, S. He, Q. Pei, Y. Li, Y. L. J. Yao, *Polym. Chem.* **2012**, *3*, 2170–2177.

12 S. W. Chiu, L. Y. Lin, H. W. Lin, Y. H. Chen, Z. Y. Huang, Y. T. Lin, F. Lin, Y. H. Liu, K. T. Wong, *Chem. Commun.* **2012**, *48*, 1857–1859.

13 E. V. Verbitskiy, E. M. Cheprakova, J. O. Subbotina, A. V. Schepochkin, P. A. Slepukhin, G. L. Rusinov, V. N. Charushin, O. N. Chupakhin, N. I. Makarova, A. V. Metelitsa, V. I. Minkin, *Dyes Pigment* **2014**, *100*, 201e214.

14 Q. Shi, P. Cheng, Y. Li, X. Zhan, *Adv. Energy Mater.* **2012**, *2*, 63–67.

15 A. Tang, L. Li, Z. Lu, J. Huang, H. Jia, C. Zhan, Z. Tan, Y. Li, J. Yao, *J. Mater. Chem. A* **2013**, *1*, 5747–5757.

16 J. H. Kim, H. U. Kim, C. E. Song, I. N. Kang, J. K. Lee, W. S. Shin, D. H. Hwang, *Sol. Energy Mater. Sol. Cells* **2013**, *108*, 113–125.

17 T. H. Lee, K. Y. Wu, T. Y. Lin, J. S. Wu, C. L. Wang, C. S. Hsu, *Macromolecules* **2013**, *46*, 7687–7695.

18 V. Tamilavan, J. B. Park, I. N. Kang, D. H. Hwang, M. H. Hyun, *Synth. Met.* **2014**, *198*, 230–238.

19 L. Huo, S. Zhang, X. Guo, F. Xu, Y. Li, J. Hou, *Angew. Chem. Int. Ed. Engl.* **2011**, *50*, 9697–9702.

20 A. Gadisa, M. Svensson, M. R. Andersson, O. Inganns, *Appl. Phys. Lett.* **2004**, *84*, 1609–1611.

21 M. Y. Jo, S. J. Park, T. Park, Y. S. Won, J. H. Kim, *Org. Electron.* **2012**, *13*, 2185–2191.

22 M. C. Scharber, D. Mühlbacher, M. Koppe, P. Denk, C. Waldauf, A. J. Heeger, C. J. Brabec, *Adv. Mater.* **2006**, *18*, 789–794.

23 J. H. Kim, C. E. Song, B. S. Kim, I. N. Kang, W. S. Shin, D. H. Hwang, *Chem. Mater.* **2014**, *26*, 1234–1242.

24 M. J. Frisch, G. W. Trucks, H. B. Schlegel, G. E. Scuseria, M. A. Robb, J. R. Cheeseman, J. A. Montgomery, T. Vreven, K. N. Kudin, J. C. Burant, J. M. Millam, S. S. Iyengar, J. Tomasi, V. Barone, B. Mennucci, M. Cossi, G. Scalmani, N. Rega, G. A. Petersson, H. Nakatsuji, M. Hada, M. Ehara, K. Toyota, R. Fukuda, J. Hasegawa, M. Ishida, T. Nakajima, Y. Honda, O. Kitao, H. Nakai, M. Klene, X. Li, J. E. Knox, H. P. Hratchian, J. B. Cross, V. Bakken, C. Adamo, J. Jaramillo, R. Gomperts, R. E. Stratmann, O. Yazyev, A.J. Austin, R. Cammi, C. Pomelli, J. W. Ochterski, P. Y. Ayala, K. Morokuma, G. A. Voth, P. Salvador, J. J. Dannenberg, V. G. Zakrzewski, S. Dapprich, A. D. Daniels, M. C. Strain, O. Farkas, D. K. Malick, A. D. Rabuck, K. Raghavachari, J. B. Foresman, J. V. Ortiz, Q. Cui, A. G. Baboul, S. Clifford, J. Cioslowski, B. B. Stefanov, G. Liu, A. Liashenko, P. Piskorz, I. Komaromi, R. L. Martin, D. J. Fox, T. Keith, M. A. Al-Laham, C. Y. Peng, A. Nanayakkara, M. Challacombe, P. M. W. Gill, B. Johnson, W. Chen, M. W. Wong, C. Gonzalez, J. A. Pople, Gaussian 03, Revision E.01; Gaussian Inc.: Wallingford, CT, **2004**.

25 K. Reichenbaecher, H. I. Suess, J. Hulliger, *Chem. Soc. Rev.* **2005**, *34*, 22–30

26 Y. Wang, M. D. Watson, *Macromolecules* **2008**, *41*, 8643–8647.

27 H. H. Cho, T. E. Kang, K. H. Kim, H. Kang, H. J. Kim, *Macromolecules* **2012**, *45*, 6415–6417. -

28 J. H. Kim, C. E. Song, N. Shin, H. Kang, S. Wood, I. N. Kang, B. J. Kim, B. S. Kim, J. S. Kim, W. S. Shin, D. H. Hwang, *ACS. Appl. Mater. Interfaces* **2013**, *5*, 12820–12831.